applied sciences

MDPI

Article

Scalable Fabrication of Si-Graphene Composite as Anode for Li-ion Batteries

Ding Lou [1], Shuyi Chen [2], Strauss Langrud [3], Amir Abdul Razzaq [3], Mingyang Mao [1], Hammad Younes [4,*], Weibing Xing [3], Tim Lin [2,5] and Haiping Hong [4,*]

[1] Department of Nanoscience and Nanoengineering, South Dakota School of Mines and Technology, Rapid City, SD 57701, USA
[2] Solid Energies, Inc., 985 E Orangefair Ln, Anaheim, CA 92801, USA
[3] The Energy Storage Lab, Department of Mechanical Engineering, South Dakota School of Mines and Technology, Rapid City, SD 57701, USA
[4] Department of Electrical Engineering, South Dakota School of Mines and Technology, Rapid City, SD 57701, USA
[5] Bioenno Tech, LLC, 3657 McFadden Ave, Santa Ana, CA 92704, USA
* Correspondence: hammad.younes@sdsmt.edu (H.Y.); haiping.hong@sdsmt.edu (H.H.); Tel.: +1-(605)-863-7261 (H.Y.); +1-(605)-431-7642 (H.H.)

Abstract: A facile and scalable method is reported to fabricate Si-graphene nanocomposite as anode material for Li-ion batteries (LIBs) with high capacity and capacity retention performance. The Si-graphene electrode showed an initial discharge capacity of 1307 mAh g^{-1} at a current rate of 0.1C. At the 25th cycle, the electrode retained a discharge capacity of 1270 mAh g^{-1}, with an excellent capacity retention of 97%. At the 50th cycle, the electrode still retained high capacity retention of 89%. The improved capacity retention of Si-graphene anode compared with Si anode is attributed to the mechanical flexibility of graphene that compromises the volume expansion of Si during the lithiation/delithiation process. The electrochemical impedance measurement further confirms the enhanced electrical conductivity and the denser solid-electrolyte-interface of the Si-graphene electrode. This fabrication approach is cost-effective and easy to scale up compared to known techniques, making it a promising candidate for commercializing Si-based anode for LIBs.

Keywords: Si-graphene electrode; Li-ion batteries; anode; scalable

Citation: Lou, D.; Chen, S.; Langrud, S.; Razzaq, A.A.; Mao, M.; Younes, H.; Xing, W.; Lin, T.; Hong, H. Scalable Fabrication of Si-Graphene Composite as Anode for Li-ion Batteries. *Appl. Sci.* **2022**, *12*, 10926. https://doi.org/10.3390/app122110926

Academic Editor: José Miguel Campiña Pina

Received: 23 September 2022
Accepted: 27 October 2022
Published: 28 October 2022

1. Introduction

The need for lithium-ion batteries (LIBs) with higher energy density and longer cycle life has significantly increased due to the increased demands for electric vehicles and portable electronics [1–5]. Graphite and activated carbon have been used for long time to fabricate batteries. However, graphite with limited theoretical capacity of (370 mAh g^{-1}) is still a big challenge [6]. Activated carbon have high electrical conductivity with large surface area. However, the large specific surface area materials might be rich with micropores, blocked pores, and dead-end pores, which provide a high surface area but are hard to be accessed by the ions [7]. These facts are evidence that the high surface area is not the key for the high theoretical capacity. Therefore, the material must have a high surface area due to large mesopore volume to obtain a high theoretical capacity. To further boost the actual energy density of LIBs, silicon (Si), with a theoretical capacity of 3579 mAh g^{-1}, has been used as a promising anode material for next-generation LIBs with higher power and energy storage capacity [6,8,9]. However, the low intrinsic electrical conductivity of Si, along with the volume expansion of up to 400% during the lithiation/delithiation process, are causing severe mechanical disintegration such as pulverization that results in poor electrical contact with the conductive phase and eventually leads to the degradation of the electrodes and limited cycle life [10,11]. Therefore, several novel approaches have been

explored to overcome Si anode materials' critical volume change issue to meet satisfactory cycling performance [12].

Graphene is a promising material to improve the electrochemical performance of Si anode because of its high electrical conductivity and 2D layered structure that can solve the problem of the significant volume change of Si [13,14]. Specific structures of Si/Graphene have been explored, such as core–shell structure and Si/graphene foil structure [13,15,16]. The freestanding Li_xSi/graphene reported by Zhao et al. with a unique foil structure, where graphene sheets entirely encapsulated Li_xSi nanoparticles were stable in different air conditions and yielded 98% capacity retention after 400 cycles [15]. The silver-coated Si/graphene core/shell fiber structure fabricated by wet-spinning showed significantly improved electrochemical performance due to the structural integrity of double-locked graphene layers [17]. Recently, Zhang et al. synthesized Si/graphene composite through ball-milling technique. The Si nanoparticles and the graphene nanosheets were firstly functionalized with amino and carboxyl groups, respectively, in order to obtain covalent interactions, followed by a ball-milling process where the functionalized Si and graphene self-assembled. The as-prepared composite exhibited stable cycling performance after 500 cycles due to the graphene sheets successfully encapsulated Si nanoparticles on their surfaces. The reported synthesis route has the potential to be scaled up and extended to fabricate Si anode for commercialization of LIB electrodes [18].

However, the challenge arises as graphene easily forms agglomerates due to the high van der Waals interactions [19]. One of the common ways to overcome such a challenge is to apply a binder between the graphene sheets. The Si/Nitrogen(N)-doped graphene pomegranate-like structure constructed by Si nanoparticles surrounded by N-doped graphene sheets was successfully synthesized and showed remarkable capacity retention [20,21]. Sulfur (S) has also been used to dope the graphene sheets, as reported by Hassan et al., who introduced a new design of wrapping Si nanoparticles with S-doped graphene sheets and then shielding the Si/S-doped graphene composite with polyacrylonitrile (PAN) [22]. Lee et al. modified Si nanoparticles with a thin polyaniline layer and obtained well-dispersed Si into graphene sheets using supercritical carbon dioxide ($scCO_2$). The fabricated composite showed superior capacity performance which was attributed to the graphene sheets and the polyaniline shell that was polymerized on the Si nanoparticles. the synthesized graphene-polyaniline-Si framework provided excess space to tolerate the volume change of Si and in the meantime promote the diffusion of Li ions [23]. Bai's group synthesized a porous 3D graphene hydrogel (GH) composite embedded with an ultrathin SiO_x layer coated Si nanoparticles. The fabricated composite ($Si@SiO_x$/GH) showed remarkable storage capacity and good capacity retention of 80% at 140th cycle [24].

Graphene and reduced graphene oxide (rGO) have been extensively investigated to synthesize composite anode materials in various ways to explore better electrochemical performance [25–28]. Due to the large specific area and great mechanical flexibility, it was reported that rGO not only provided a porous graphene-like structure for compromising the volume change of Si and maintaining the structure of the anode materials but also served as a binder that can form chemical bonds with OH functionalized Si nanoparticles [10,25,29]. Instead of simply wrapping rGO around the Si nanoparticles by physical mixing, which usually leads to failure of stable cycling performance despite the good contact between Si and rGO, researchers have designed to introduce a second carbon phase such as amorphous carbon to achieve better cycling performance of Si anode materials [30,31]. Feng et al. presented a freeze-drying method, followed by a subsequent chemical vapor deposition (CVD) to synthesize the Si-rGO-C composite, which created a conductive network to maintain the contact between the current collector and the electrode [31,32]. Another alternative method to prepare Si/rGO composite anode material is the in situ reduction or decomposition of Si precursors such as silicon dioxide (SiO_2), preventing Si nanoparticles from agglomerating [33]. Wu et al. presented a step-by-step synthesis of fabricating Si-loaded 3D graphene composite by in situ magnesiothermic reduction of SiO_2@Graphene [34]. The produced

Si@Graphene composite yielded a superior specific capacity of 500 mAh g^{-1} at a current density of 20 A g^{-1}. Yao's group designed a porous Si nanofilm growing on both sides of rGO sheets by in situ reduction of SiO_2-rGO-SiO_2. The resultant Si-rGO-Si composite was then coated by a carbon layer, forming a stable solid electrolyte interface (SEI). The electrode made of this carbon-coated Si composite showed a remarkable specific capacity of 894 mAh g^{-1} after 1000 cycles at 1 A g^{-1} [35].

However, the reported approaches of fabricating Si/graphene electrode require either multistep synthesis or complex surface modification, despite the enhanced capacity performance that has been achieved [30,31,34]. It is essential to develop an efficient and cost-effective route of fabricating Si/graphene compound to meet the needs of potential commercialization.

In this article, we report a simple and scalable method of fabricating Si-graphene nanocomposite as an anode material for LIB by uniformly dispersing Si and graphene nanoparticles in liquid media with the aid of an appropriate surfactant. The idea was prompted from our previous research in the field of nanofluids, where we developed novel "nanosolids" through the use of surfactants in aqueous media [36–38]. In this work, the assistance of the surfactant results in the homogeneous distribution of graphene nanosheets with Si nanoparticles firmly attached to them, that significantly enhances the cross-layer electron transportation and compromises the volume expansion of Si nanoparticles during the lithiation/delithiation process. Besides, the graphene nanosheets provide an efficient path for the Li ions, which is essential for high capacity and cycling performance [23]. This fabrication approach is cost-effective and easy to scale up compared to known techniques, making it a promising candidate for commercializing Si anode materials for LIBs [39].

2. Materials and Methods

2.1. Synthesis of Si-Graphene Nanocomposite

Graphene nanoplatelets (Cheap Tubes Inc., Grafton, VT, USA), Grade 3, prepared by acid exfoliation, are multilayer graphene (4–5 layers) with a thickness of 8 nm, a purity >97%, and a surface area of 600–750 m^2 g^{-1}. Sodium dodecylbenzenesulfonate (SDBS) was purchased from Sigma Aldrich and functioned as a surfactant. Silicon Nanopowder (Si, 98+%, 50–70 nm, laser synthesized, polycrystalline structure) was purchased from US Research Nanomaterials, Inc., Huston, TX, USA. All the materials were used as received, without any pre-treatment.

Briefly, the surfactant SDBS, graphene, and Si nanoparticles were sequentially dispersed in deionized water (DI water) with concentrations of 2.0 wt.%, 0.2 wt.%, and 0.2 wt.%, respectively. The dispersion was obtained using ultrasonication (Branson Model 450 Digital Sonifier with a 3/4″ disrupter horn). The power of the ultrasonication was set at 20% amplitude (about 40 watts) and the sonication time for each material is 20 min. During the dispersion of Si nanopowders, an ice bath was used to maintain the temperature of the fluid. After that, the fluid was transferred to a vacuum-assisted filtration setup and repeatedly washed with DI water to remove the excess surfactant. The filtered solid mixture was then taken out of the funnel and left in a vacuum oven at 80 °C for 12 h. The dried sample was then scraped off the filter and ground with a marble pestle and mortar. Figure 1 shows the schematic diagram of the preparation of the Si-graphene nanocomposite.

2.2. Characterization

Scanning electron microscope (SEM) images were obtained using a Thermo Fisher Scientific (Waltham, MA, USA) Helios™ 5 DualBeam SEM equipped with an Oxford™ AZtecEnergy advanced system for Energy-dispersive X-ray spectroscopy (EDS). Raman spectroscopy (Foster+Freeman Foram®, Foster+Freeman Ltd., Evesham, WR, United Kingdom) and X-ray diffraction (XRD) (Malvern Panalytical Empyrean X-ray diffractometer equipped with a pixel 3D detector, Malvern Panalytical Ltd., Malvern, WR, United Kingdom) were used to characterize the fabricated Si-graphene composite.

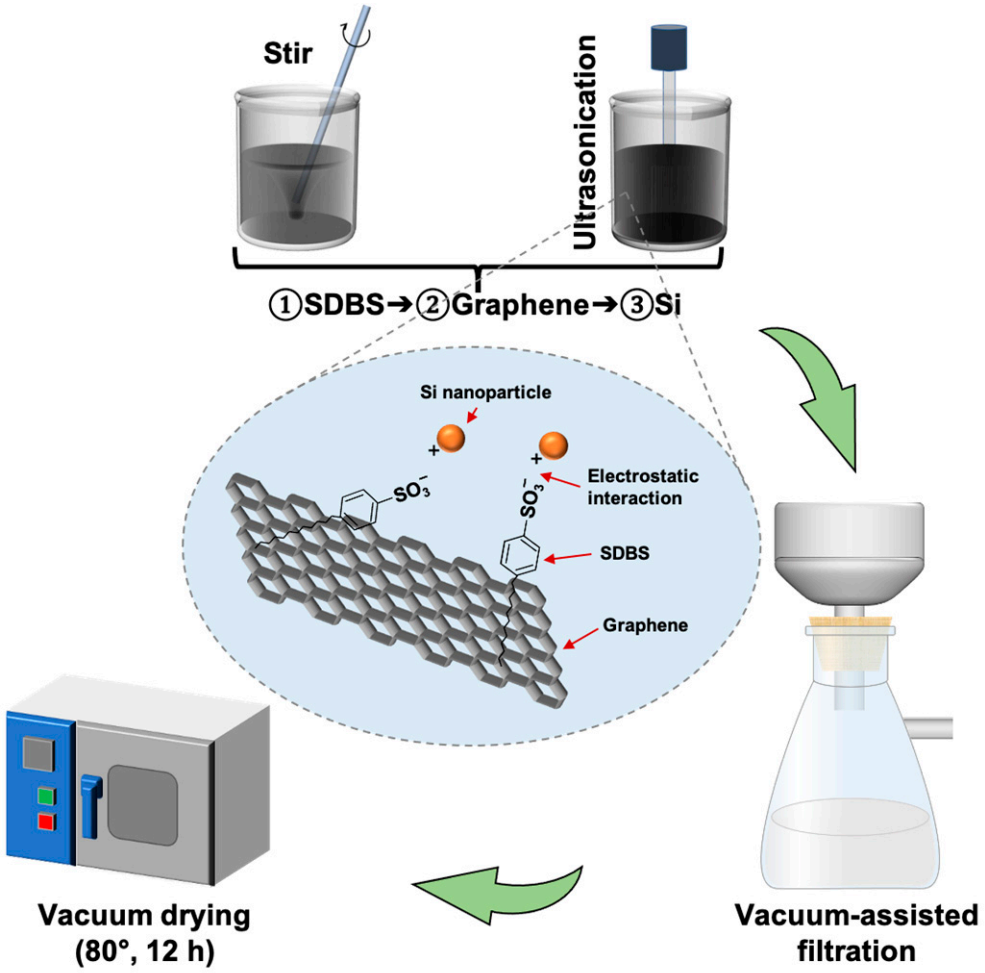

Figure 1. Schematic diagram of the preparation of Si-graphene nanocomposite.

2.3. Coin Cell Fabrication

The Si-graphene electrode was comprised of 80 wt.% active material (Si-graphene, 50/50 weight ratio) and 20 wt.% poly(acrylic acid) binder (PAA, 25 wt.% solutions in water, Alfa Aesar, Ward Hill, MA, USA). An additional conductive agent is not involved. As a comparison, a Si nanoparticle-based electrode was also prepared, which comprised of 40 wt.% Si nanopowder, 40 wt.% conductive agents (acetylene carbon black, 99.9%, Alfa Aesar), and 20 wt.% PAA as the binder. The weight ratio between Si and acetylene carbon black was 50/50. The electrode was fabricated using a typical slurry method. The slurry was mixed on a magnetic stirrer (Corning, Glendale, AZ, USA) at 800 rpm for 18 h before coating onto the copper foil (9 µm, MSE Supplies, Tucson, AZ, USA) with a micrometer-controlled doctor blade (MSK-AFA-HC100, MTI Corporation, Richmond, CA, USA) with a blade gap of 30 µm. The coated copper foil was dried in an oven at 100 °C for 2 h for the solvent to evaporate. The dried coatings were then transferred into a vacuum oven that was set to 120°C for an overnight period before the coin cell assembly. The weight percentage of the active material was ~1 mg cm^{-2}. 2032-type coin cells were used with the Li foil (0.6 mm thickness, Sigma-Aldrich, St. Louis, MO, USA) as the counter electrode and a PP membrane (Celgard 3501) as the separator. The cells were filled with 1.0 M LiPF6 in EC/DEC = 1/1 (*v*/*v*) (Sigma-Aldrich) as the electrolyte. The coin cells were assembled in an argon-filled glove box to avoid moisture and oxygen exposure (H_2O < 0.1 ppm, O_2 < 0.1 ppm).

2.4. Electrochemical Performance

The half cells were galvanostatically cycled between 50 mV and 0.7 V vs. Li^+/Li on a battery analyzer (MTI, BST8-MA) with a fixed C-rate at C/20 (0.06 A g^{-1}) for the formation cycle, followed by repeated cycling at C/10 (0.12 A g^{-1}). For the coin cell with Si-graphene electrode, the specific capacities were calculated based on the total mass of Si-graphene in the cell (e.g., the specific discharge capacity = discharge capacity/total weight of Si-graphene in the cell). The electrode was weighed before the cell assembly. After deducting the weight of the corresponding current collector, the Si-graphene weight ratio (80%) was applied to calculate the weight of the actual active material in the cell. Electrochemical Impedance Spectroscopy (EIS) was performed utilizing the Corrtest Instruments Corp. (Wuhan, China) model CS310 in the frequency range of 1.00 mHz to 100 kHz. The cell voltages were 1.34 V and 0.47 V for Li/Si-Graphene and Li/Si coin cells, respectively. Due to the steep voltage profiles at the voltage range, the cells were at the equivalent, fully charged state. The AC voltage amplitude was 10.0 mV.

3. Results and Discussions

Figure 1 illustrates the schematic diagram of synthesizing Si-graphene nanocomposite in aqueous solutions by utilizing SDBS surfactant. During the sonication, SDBS surfactant was first dissolved in DI water. When graphene nanosheets were added and ultrasonication was applied, the carbon chain of SDBS was attracted to the surface of the graphene sheets by van der Waals forces and π-π interactions. After Si nanoparticles were dispersed in the fluid, the Si nanoparticles yielded a positive zeta potential that tend to attract negatively charged particles. That being, the Si nanoparticles would be electrostatically attracted to the negatively charged SDBS surfactant particles which were attached to graphene sheets. Therefore, the insoluble graphene nanosheets and the Si nanoparticles were uniformly dispersed in water by simply adding the SDBS surfactant. The morphology of the as-received Si nanoparticles, graphene nanosheets, and the fabricated Si-graphene composite was characterized by scanning electron microscopy (SEM), as shown in Figure 2. The average diameter of the spherical Si nanoparticles was confirmed to range from 50–70 nm. Figure 2b shows that the lateral dimension of the graphene nanosheets varies from 50 to 150 nm, indicating the relatively low quality of the material. However, the thickness of the graphene sheets is about a few nanometers, which is beneficial for applications that require high specific surface area and electrical conductivity. Figure 2c,d are the SEM images of the fabricated Si-graphene composite. The Si nanoparticles were successfully attached to the graphene nanosheets by utilizing SDBS surfactant in the aqueous media. The red arrows in Figure 2d highlight the graphene nanosheets, and it is confirmed that the uniform dispersion of Si nanoparticles and graphene nanosheets was obtained. The tight connections between Si nanoparticles and graphene nanosheets indicate that it is efficient to utilize SDBS surfactant to provide sufficient electrostatic interactions. It is anticipated that the enhanced electrochemical performance of the Si-graphene electrode is attributed to the structural flexibility of graphene that accommodates the volume expansion of Si nanoparticles. EDS mapping (see Figure 3) was performed to verify the composition of the fabricated Si-graphene compound. The results confirm that the Si nanoparticles and the graphene nanosheets were uniformly distributed by the use of SDBS surfactant, which contains sulfur (S) and oxygen (O) elements. It is concluded to be an efficient and facile way of utilizing surfactant to homogeneously disperse Si nanoparticles and graphene nanosheets through electrostatic interactions.

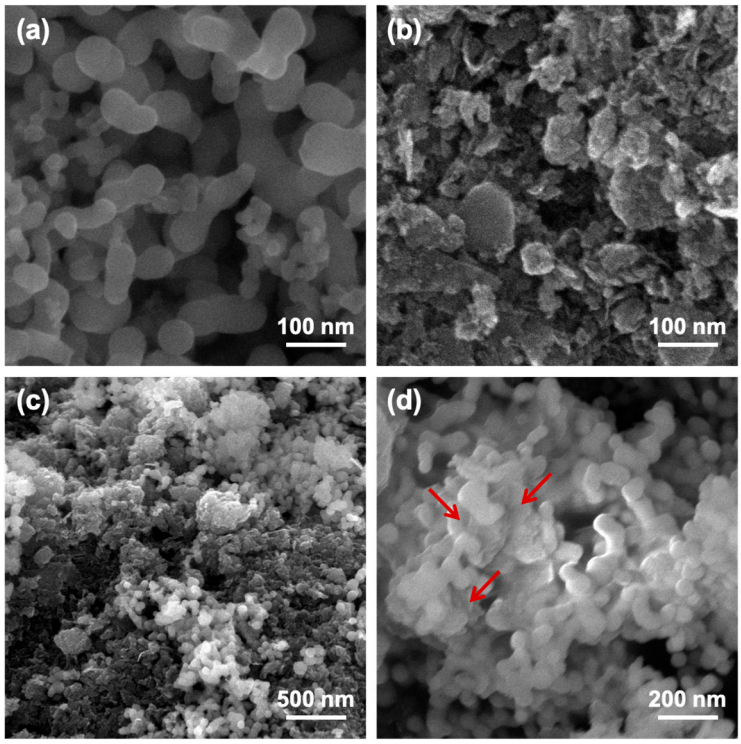

Figure 2. SEM images of (**a**) Si nanoparticle; (**b**) graphene; (**c**,**d**) Si-graphene (the red arrows highlight the graphene nanosheets).

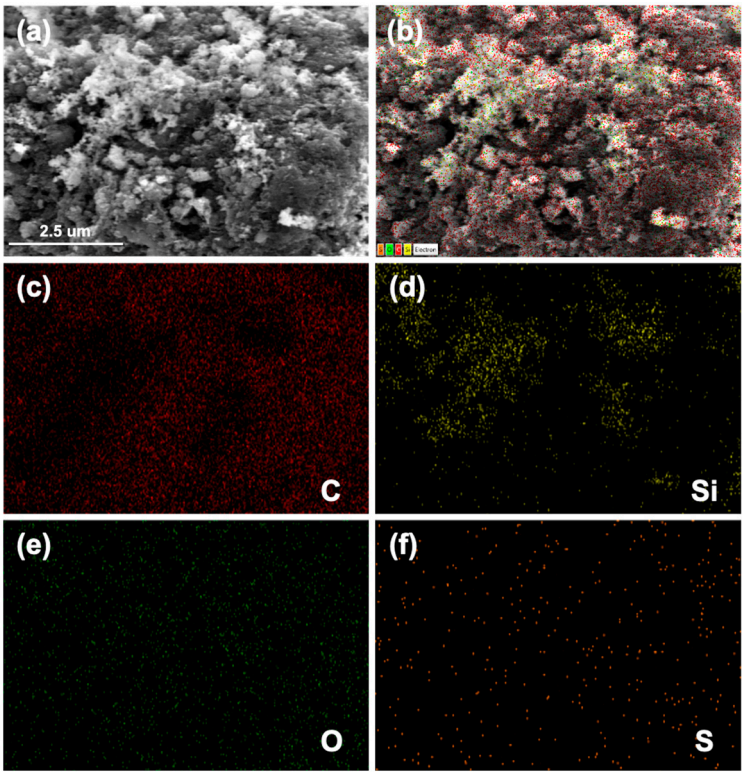

Figure 3. (**a**) SEM image of Si-graphene; EDS mapping of Si-graphene (**b**), element C (**c**), element Si (**d**), element O (**e**), and element S (**f**).

The crystalline structures of Si nanoparticle and the fabricated Si-graphene nanocomposite were characterized by XRD using a Cobalt source (λ = 0.1789 nm) (see Figure 4a). The XRD spectrum shows characteristic peaks of Si nanoparticle at 33.2°, 55.5°, 66.2°, and

82.4°, referring to the (111), (220), (311), and (400) planes of cubic Si that matches PDF 27-1402. The broad and weak peak at 30° is the reflection of the graphene. The broad diffraction peak indicates that the graphene sheets in the stack direction are not well ordered, meaning the graphene sheets were well dispersed with Si nanoparticles. Figure 4b shows the Raman spectra of Si, graphene and Si-graphene composite. The characteristic peak around 520 cm^{-1} indicates Si nanoparticle, and the other two peaks at around 1335 cm^{-1} and 1575 cm^{-1} are the D and G peaks of graphene, corresponding to the vibration of sp^3 defects-induced and sp^2 bonded carbon atoms. The intensities of the D and G peaks in the Si-graphene composite are similar, indicating the graphene possesses many defects that could provide extra diffusion paths for Li ions. In addition, the significantly reduced 2D band in Si-graphene composite indicate that the multilayer graphene structure is gone, which further confirms the homogeneous distribution of the Si nanoparticles and the graphene nanosheets.

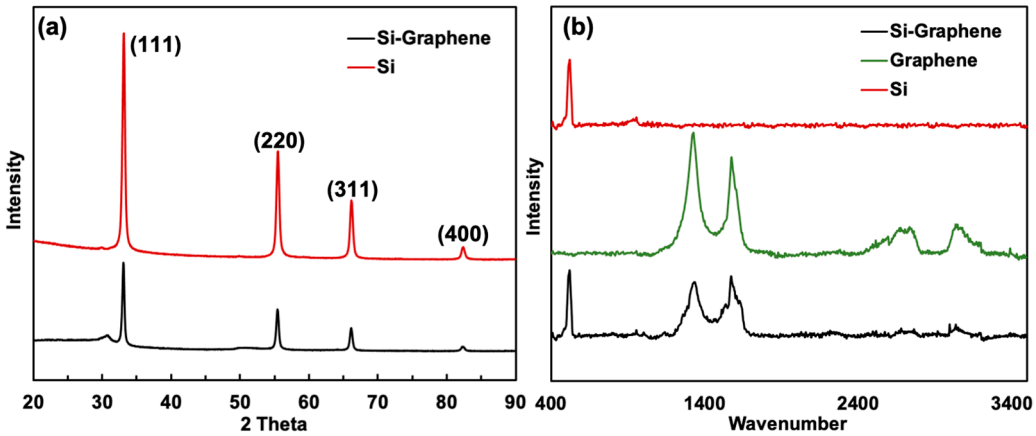

Figure 4. (**a**) XRD patterns of Si nanoparticle and Si-graphene composite; (**b**) Raman spectra of Si, graphene and Si-graphene composite.

A coin cell with a lithium electrode was used to measure the charge/discharge capacities of the Si-graphene composite electrode. For comparison, a coin cell composed of lithium electrode and Si-based electrode was fabricated and evaluated. The specific charge and discharge capacities were calculated based on the total weight of the Si-graphene composite used to fabricate the half cell. Figure 5a shows the specific charge and discharge capacities of Si-graphene and Si anodes at a current rate of 0.05C. As expected, the Si-based coin cell shows a much higher specific capacity than the Si-graphene composite coin cell for the initial cycle. This is due to the intrinsic high capacity of the Si nanoparticles. Figure 5b shows the specific charge and discharge capacities of Si-graphene anode at different current rates of 0.05C, 0.1C, and 0.5C, respectively, with a voltage ranging from 0.05 to 0.7 V. The initial specific discharge capacity and charge capacity of the formation cycle were 1393 mAh g^{-1} and 1180 mAh g^{-1} at 0.05C, respectively. Therefore, the coulombic efficiency (CE = charge capacity/discharge capacity) was calculated to be 84.7%. After the formation cycle, the Si-graphene coin cell yielded discharge capacities of 1307 mAh g^{-1} at 0.1C and 433 mAh g^{-1} at 0.5C, and charge capacities of 1313 mAh g^{-1} at 0.1C and 513 mAh g^{-1} at 0.5C. Therefore, the columbic efficiencies were calculated to be 100.5% at 0.1C, and 118.5% at 0.5C. It is noticed that the capacity decays slightly faster when the cell was tested at a lower current rate. This might be due to the smaller volume expansion of the Si nanoparticles at relatively higher current rates, at which the transportation rate of the Lithium ions is relatively slower, resulting in a more stable SEI layer that prevents the irreversible loss of capacity. The energy density of the Si-graphene active material at 0.1C was calculated to be 522.8 Wh kg^{-1} using Equation (1).

$$\text{Energy density} = C * V \quad (1)$$

where C is the specific discharge capacity (1307 mAh g^{-1} at 0.1C), V is the voltage at 50% state of charge (0.4 V in this case).

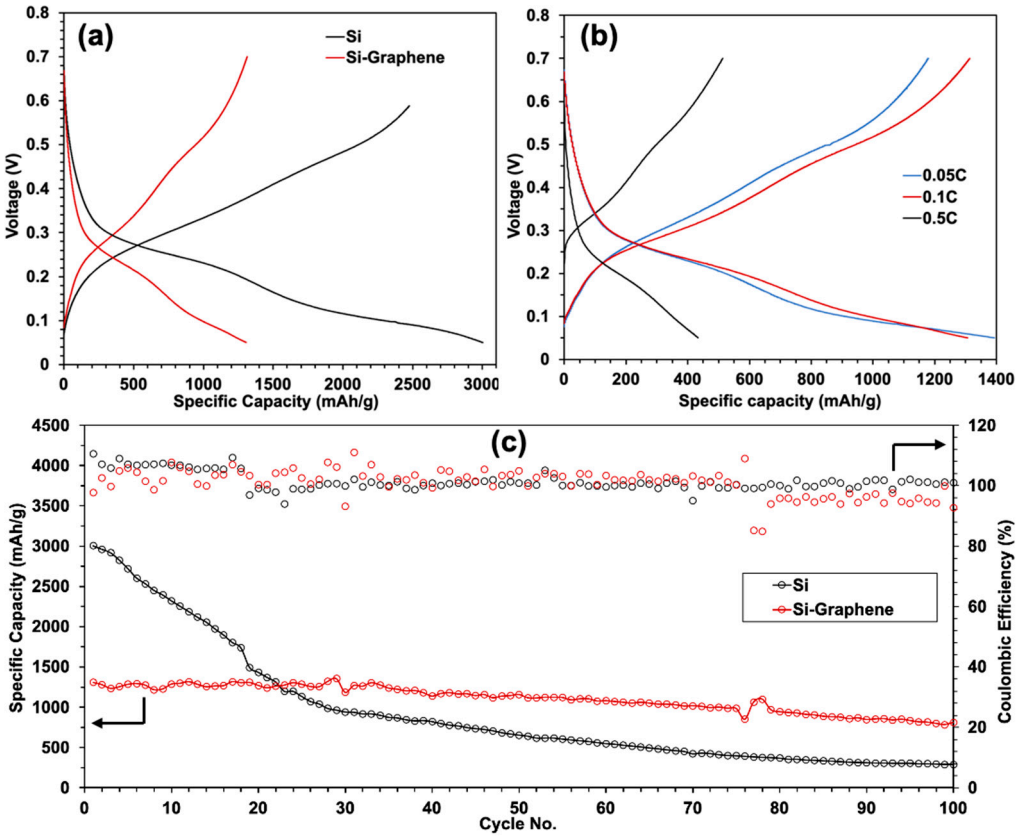

Figure 5. (**a**) Specific charge/discharge capacity of Si-graphene and Si anodes at 0.05C; (**b**) specific charge/discharge capacity of Si-graphene anode at 0.05C, 0.1C, and 0.5C, respectively; (**c**) specific charge/discharge cycling performance of Si-graphene and Si anodes at a current rate of 0.1C in the first 100 cycles.

Figure 5c shows the cycle performance of the Si-graphene electrode and the Si electrode at a current rate of 0.1C. The Si-graphene electrode showed an initial discharge capacity of 1307 mAh g^{-1} at a current rate of 0.1C. At the 25th cycle, the electrode retained a discharge capacity of 1270 mAh g^{-1}, with an excellent capacity retention of 97%. At the 50th cycle, the electrode still retained high capacity retention of 89%. As a comparison, the pure Si anode possessed a higher initial discharge capacity (over 3000 mAh g^{-1} at 0.1C), while the decay of the capacity retention was much faster, because Si nanoparticles experienced dramatic volume change during the charge/discharge process which ultimately led to limited cycle life. The enhanced cycling stability of the Si-graphene electrode was mainly attributed to the graphene structure that accommodates the volume expansion of the Si nanoparticles. However, the capacity fading became faster beyond 50 cycles. At the 100th cycle, the electrode delivered a specific discharge capacity of 810 mAh g^{-1} with 62% retention. Although the specific capacity decreases at long cycles, it is noticed that the columbic efficiencies obtained were all over 90%, indicating a stable structure of the solid electrolyte interface. It is noticed that the columbic efficiencies exceeded 100% at several points, which could be attributed to the uncontrolled temperature during the half-coin cell test. A relatively higher room temperature during the discharge process would deliver a discharge capacity that is higher than the charge capacity, resulting in the columbic efficiency going beyond 100%. Conclusively, the improved capacity retention of the Si-graphene anode is attributed to the uniform distribution of Si nanoparticles and

graphene nanosheets, although the initial specific capacity is decreased due to the intrinsic low capacity of graphene.

To further understand the improved performance of the Si-graphene electrode compared to pure Si anode, electrochemical impedance spectroscopy (EIS) was performed, and the Nyquist plots for both electrodes are shown in Figure 6. It is seen from Figure 6 that the Si-based coin cell showed a higher electrochemical resistance than the Si-graphene composite coin cell. An equivalent circuit (see insert of Figure 6a) was used to fit the EIS plots, where R_0 is the bulk resistance, CPE is constant phase element, $CPE_1||R_1$ is assigned to interfacial electrode/electrolyte charge transfer impedance, $CPE_2||R_2$ is assigned to SEI layer at the lithium anode surface, and W represents a Warburg (mass transfer) impedance at low frequency. The EIS parameters after fitting the EIS plots to the equivalent circuit are summarized in Table 1. The charge transfer resistance R_1 of the Si-Graphene based cell (224 Ω) is 40% lower than that of the Si-based cell (355 Ω), as shown in Table 1, which indicates faster electrochemical conversion reaction kinetics of the Li/Si-graphene cell as compared to the Li/Si cell. This is because of the excellent electrical conductivity of graphene nanosheets. The bulk resistance R_0 and the SEI resistance R_2 of the Si-graphene based cell are lower than those of the Si-based cell, as shown in Table 1, suggesting the higher electrode conductivity and the denser SEI layer of the Si-graphene based cell than the Si-based cell. In addition, the reduced Warburg resistance of the Si-graphene composite coin cell indicates the enhanced mass transfer activity of Li ions, which promotes the electrochemical performance. The electrochemical impedance measurements further confirm that the improved performance of the Si-graphene anode is attributed to the graphene nanosheets that tolerate the volume change of Si nanoparticles and increase the electrical conductivity.

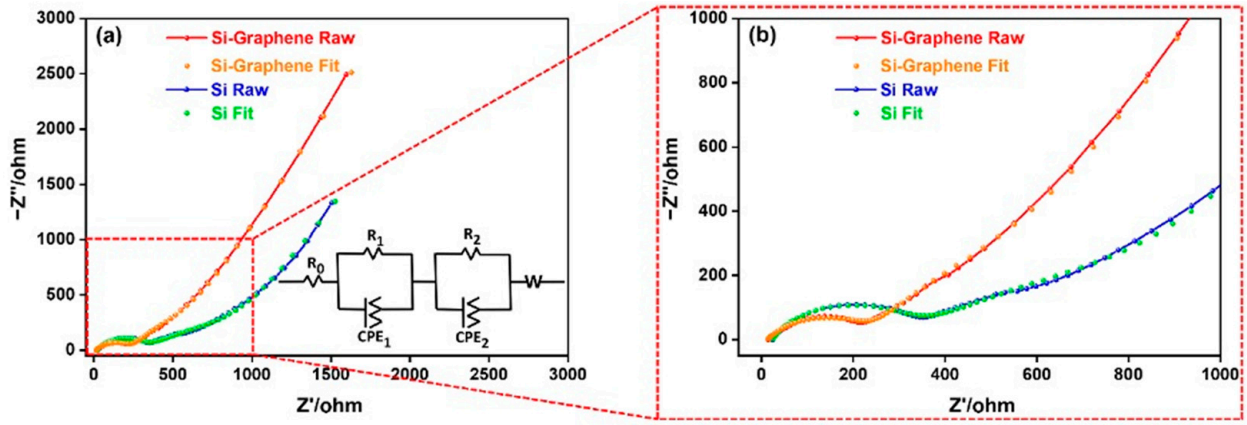

Figure 6. (**a**) Full-scale and (**b**) magnified EIS spectra of Li/Si and Li/Si-graphene coin cells.

Table 1. EIS parameters of the Li/Si and Li/Si-graphene coin cells.

EIS Parameter	R_0 (Ω)	R_1 (Ω)	R_2 (Ω)
Si	23.4	355	206
Si-graphene	12.9	224	183

4. Discussions

With the rapid development of advanced technology, there is huge and increasing needs for Li ion batteries with high performance. Compared to other carbon nanomaterials such as carbon nanotubes or nanofibers [40,41], graphene nanosheet and its derivatives have attracted more attention in the fabrication of Si-based anodes mainly due to the 2D layered structure that can better tolerate the volume expansion of Si nanoparticles [42]. However, the reported approaches of fabricating Si/graphene electrode require either multistep synthesis or complex surface modification, despite the enhanced capacity per-

formance that has been achieved [30,31,34]. The commercialization of Si-based anode materials requires cost-effective and scalable synthesis. Table 2 summarizes the synthesis techniques/conditions and capacity performance of various Si/graphene anodes from literature published in the recent years. Compared to other publications, the Si-graphene anode reported in this work did not show significant improvement in capacity performance. However, the synthesis techniques and conditions in this work are much easier than other reported methods. The Si nanoparticles are electrostatically attached to graphene nanosheets by utilizing SDBS surfactant. This facile and cost-effective method of uniformly dispersing nanoparticles, prompted from the authors' previous research in the field of nanofluids, can potentially lead to advanced commercialization of anode materials for LIBs. Despite the unsatisfying results, the authors believe that the fabrication approach reported in this work is worth exploring in the future. The capacity performance could be boosted in further research by improving the quality of the graphene, reducing the amount of the surfactant, or optimizing the synthesis procedure.

Table 2. Synthesis and capacity performance of Si/graphene related anodes from literature.

Ref.	Anode Material	Synthesis Techniques/Conditions	Capacity Performance
[21]	Si-graphene	Aerosol spray process, atomize at 450 °C, thermal annealing up to 800 °C, autoclave at 650 °C, CVD at 900 °C, impurity wash off.	890 mAh g^{-1} at 5 A g^{-1}; 81.9% retention after 150 cycles at 1 C (135 mA g^{-1}).
[30]	Carbon-coated Si/graphene framework	Synthesis of GO by m-Hummers method, hydrothermal reaction at 180 °C, freeze-drying, thermal treatment at 800 °C.	830 mAh g^{-1} at 1 A g^{-1}; 85.1% retention after 200 cycles at 1 A g^{-1}.
[31]	Si/rGO/C	Synthesis of GO by m-Hummers method, freeze-drying, CVD at 900 °C.	894 mAh g^{-1} at 1 C; 94% retention after 300 cycles at 1 C (1.4 A g^{-1}).
[34]	Si-3D graphene	Synthesis of GO by m-Hummers method, thermal reduction of SiO_2/GO at 800 °C, synthesis of Si/3D graphene via molten-salt-assisted magnesiothermic reduction at 700 °C, removal of unreacted SiO_2 using 5% hydrofluoric acid.	1200 mAh g^{-1} at 1 A g^{-1}; 90.9% retention after 100 cycles at 1 A g^{-1}.
This work	Si-graphene	Surfactant-assisted ultrasonication, vacuum-assisted filtration	1307 mAh g^{-1} at 0.1 C; 89% retention after 50 cycles at 0.1 C (120 mA g^{-1}).

5. Conclusions

We report a cost-effective and scalable method to fabricate Si-graphene nanocomposite as anode material for Li-ion batteries with high capacity and capacity retention performance. The fabrication procedure enables the uniform distribution of Si nanoparticles and graphene nanosheets in aqueous media by utilizing SDBS surfactants. The improved capacity retention of Si-graphene anode compared with Si anode is attributed to the mechanical flexibility of graphene that compromises the volume expansion of Si during the lithiation/delithiation process. The Si-graphene electrode showed an initial discharge capacity of 1307 mAh g^{-1} at a current rate of 0.1C. At the 25th cycle, the electrode retained a discharge capacity of 1270 mAh g^{-1}, with an excellent capacity retention of 97%. At the 50th cycle, the electrode still retained high capacity retention of 89%. As a comparison, the pure Si anode possessed a higher initial discharge capacity (over 3000 mAh g^{-1} at 0.1C), while the decay of the capacity retention was much faster, because Si nanoparticles experienced dramatic volume change during the charge/discharge process which ultimately led to limited cycle life. In addition, the electrochemical impedance performance further confirms the enhanced electrical conductivity and the denser SEI of the Si-graphene electrode. The reported fabrication approach is cost-effective and easy to scale up compared to

known techniques, making it a promising candidate for commercializing Si anode materials for LIBs.

Author Contributions: D.L.: Methodology, investigation, writing—original draft preparation; S.C., S.L., A.A.R. and M.M.: Methodology and investigation; H.Y., W.X. and T.L.: Writing—review and editing; supervision; H.H.: Writing—review and editing, conceptualization, supervision, funding acquisition. All authors have read and agreed to the published version of the manuscript.

Funding: The authors appreciate the financial support from Army Research Lab, W911NF 19-2-0329.

Institutional Review Board Statement: Not applicable.

Informed Consent Statement: Not applicable.

Data Availability Statement: The data presented in this study are available in article.

Conflicts of Interest: The authors declare no conflict of interest.

References

1. Goodenough, J.B.; Park, K.S. The Li-ion rechargeable battery: A perspective. *J. Am. Chem. Soc.* **2013**, *135*, 1167–1176. [CrossRef]
2. Philippe, B.; Dedryvere, R.; Gorgoi, M.; Rensmo, H.; Gonbeau, D.; Edstrom, K. Improved performances of nanosilicon electrodes using the salt LiFSI: A photoelectron spectroscopy study. *J. Am. Chem. Soc.* **2013**, *135*, 9829–9842. [CrossRef] [PubMed]
3. Jumari, A.; Yudha, C.S.; Widiyandari, H.; Lestari, A.P.; Rosada, R.A.; Santosa, S.P.; Purwanto, A. SiO_2/C Composite as a High Capacity Anode Material of $LiNi_{0.8}Co_{0.15}Al_{0.05}O_2$ Battery Derived from Coal Combustion Fly Ash. *Appl. Sci.* **2020**, *10*, 8428. [CrossRef]
4. Kolosov, D.A.; Glukhova, O.E. Theoretical Study of a New Porous 2D Silicon-Filled Composite Based on Graphene and Single-Walled Carbon Nanotubes for Lithium-Ion Batteries. *Appl. Sci.* **2020**, *10*, 5786. [CrossRef]
5. Shoriat Ullah, M.D.; Seo, K. Prediction of Lithium-Ion Battery Capacity by Functional Principal Component Analysis of Monitoring Data. *Appl. Sci.* **2022**, *12*, 4296. [CrossRef]
6. Su, X.; Wu, Q.; Li, J.; Xiao, X.; Lott, A.; Lu, W.; Sheldon, B.W.; Wu, J. Silicon-Based Nanomaterials for Lithium-Ion Batteries: A Review. *Adv. Energy Mater.* **2014**, *4*, 1300882. [CrossRef]
7. Liu, X.; Liu, H.; Mi, M.; Kong, W.; Ge, Y.; Hu, J. Nitrogen-doped hierarchical porous carbon aerogel for high-performance capacitive deionization. *Sep. Purif. Technol.* **2019**, *224*, 44–50. [CrossRef]
8. Choi, J.W.; Aurbach, D. Promise and reality of post-lithium-ion batteries with high energy densities. *Nat. Rev. Mater.* **2016**, *1*, 16013. [CrossRef]
9. Liang, B.; Liu, Y.; Xu, Y. Silicon-based materials as high capacity anodes for next generation lithium ion batteries. *J. Power Sources* **2014**, *267*, 469–490. [CrossRef]
10. Gao, X.; Li, J.; Xie, Y.; Guan, D.; Yuan, C. A multilayered silicon-reduced graphene oxide electrode for high performance lithium-ion batteries. *ACS Appl. Mater. Interfaces* **2015**, *7*, 7855–7862. [CrossRef] [PubMed]
11. Jin, Y.; Tan, Y.; Hu, X.; Zhu, B.; Zheng, Q.; Zhang, Z.; Zhu, G.; Yu, Q.; Jin, Z.; Zhu, J. Scalable Production of the Silicon-Tin Yin-Yang Hybrid Structure with Graphene Coating for High Performance Lithium-Ion Battery Anodes. *ACS Appl. Mater. Interfaces* **2017**, *9*, 15388–15393. [CrossRef] [PubMed]
12. Ashuri, M.; He, Q.; Shaw, L.L. Silicon as a potential anode material for Li-ion batteries: Where size, geometry and structure matter. *Nanoscale* **2016**, *8*, 74–103. [CrossRef] [PubMed]
13. Cai, H.; Han, K.; Jiang, H.; Wang, J.; Liu, H. Self-standing silicon-carbon nanotube/graphene by a scalable in situ approach from low-cost Al-Si alloy powder for lithium ion batteries. *J. Phys. Chem. Solids* **2017**, *109*, 9–17. [CrossRef]
14. Son, I.H.; Hwan Park, J.; Kwon, S.; Park, S.; Rummeli, M.H.; Bachmatiuk, A.; Song, H.J.; Ku, J.; Choi, J.W.; Choi, J.M.; et al. Silicon carbide-free graphene growth on silicon for lithium-ion battery with high volumetric energy density. *Nat. Commun.* **2015**, *6*, 7393. [CrossRef] [PubMed]
15. Zhao, J.; Zhou, G.; Yan, K.; Xie, J.; Li, Y.; Liao, L.; Jin, Y.; Liu, K.; Hsu, P.C.; Wang, J.; et al. Air-stable and freestanding lithium alloy/graphene foil as an alternative to lithium metal anodes. *Nat. Nanotechnol.* **2017**, *12*, 993–999. [CrossRef] [PubMed]
16. Wang, M.-S.; Wang, G.-L.; Wang, S.; Zhang, J.; Wang, J.; Zhong, W.; Tang, F.; Yang, Z.-L.; Zheng, J.; Li, X. In situ catalytic growth 3D multi-layers graphene sheets coated nano-silicon anode for high performance lithium-ion batteries. *Chem. Eng. J.* **2019**, *356*, 895–903. [CrossRef]
17. Gu, M.; Ko, S.; Yoo, S.; Lee, E.; Min, S.H.; Park, S.; Kim, B.-S. Double locked silver-coated silicon nanoparticle/graphene core/shell fiber for high-performance lithium-ion battery anodes. *J. Power Sources* **2015**, *300*, 351–357. [CrossRef]
18. Zhang, Y.; Cheng, Y.; Song, J.; Zhang, Y.; Shi, Q.; Wang, J.; Tian, F.; Yuan, S.; Su, Z.; Zhou, C.; et al. Functionalization-assistant ball milling towards Si/graphene anodes in high performance Li-ion batteries. *Carbon* **2021**, *181*, 300–309. [CrossRef]
19. David, L.; Bhandavat, R.; Barrera, U.; Singh, G. Silicon oxycarbide glass-graphene composite paper electrode for long-cycle lithium-ion batteries. *Nat. Commun.* **2016**, *7*, 10998. [CrossRef]

20. Lin, J.; He, J.; Chen, Y.; Li, Q.; Yu, B.; Xu, C.; Zhang, W. Pomegranate-Like Silicon/Nitrogen-doped Graphene Microspheres as Superior-Capacity Anode for Lithium-Ion Batteries. *Electrochim. Acta* **2016**, *215*, 667–673. [CrossRef]
21. Nie, P.; Le, Z.; Chen, G.; Liu, D.; Liu, X.; Wu, H.B.; Xu, P.; Li, X.; Liu, F.; Chang, L.; et al. Graphene Caging Silicon Particles for High-Performance Lithium-Ion Batteries. *Small* **2018**, *14*, e1800635. [CrossRef] [PubMed]
22. Hassan, F.M.; Batmaz, R.; Li, J.; Wang, X.; Xiao, X.; Yu, A.; Chen, Z. Evidence of covalent synergy in silicon-sulfur-graphene yielding highly efficient and long-life lithium-ion batteries. *Nat. Commun.* **2015**, *6*, 8597. [CrossRef]
23. Lee, S.H.; Park, S.; Kim, M.; Yoon, D.; Chanthad, C.; Cho, M.; Kim, J.; Park, J.H.; Lee, Y. Supercritical Carbon Dioxide-Assisted Process for Well-Dispersed Silicon/Graphene Composite as a Li ion Battery Anode. *Sci. Rep.* **2016**, *6*, 32011. [CrossRef] [PubMed]
24. Bai, X.; Yu, Y.; Kung, H.H.; Wang, B.; Jiang, J. Si@SiOx/graphene hydrogel composite anode for lithium-ion battery. *J. Power Sources* **2016**, *306*, 42–48. [CrossRef]
25. Qin, J.; Wu, M.; Feng, T.; Chen, C.; Tu, C.; Li, X.; Duan, C.; Xia, D.; Wang, D. High rate capability and long cycling life of graphene-coated silicon composite anodes for lithium ion batteries. *Electrochim. Acta* **2017**, *256*, 259–266. [CrossRef]
26. Al Suwaidi, F.; Younes, H.; Sreepal, V.; Nair, R.R.; Aubry, C.; Zou, L. Strategies for tuning hierarchical porosity of 3D rGO to optimize ion electrosorption. *2D Mater.* **2019**, *6*, 045010. [CrossRef]
27. Aval, L.F.; Ghoranneviss, M.; Pour, G.B. High-performance supercapacitors based on the carbon nanotubes, graphene and graphite nanoparticles electrodes. *Heliyon* **2018**, *4*, e00862. [CrossRef]
28. Behzadi Pour, G.; Fekri Aval, L.; Mirzaee, M. Flexible graphene supercapacitor based on the PVA electrolyte and Ba-TiO3/PEDOT:PSS composite separator. *J. Mater. Sci. Mater. Electron.* **2018**, *29*, 17432–17437. [CrossRef]
29. Shan, C.; Wu, K.; Yen, H.J.; Narvaez Villarrubia, C.; Nakotte, T.; Bo, X.; Zhou, M.; Wu, G.; Wang, H.L. Graphene Oxides Used as a New "Dual Role" Binder for Stabilizing Silicon Nanoparticles in Lithium-Ion Battery. *ACS Appl. Mater. Interfaces* **2018**, *10*, 15665–15672. [CrossRef]
30. Zhang, F.; Yang, X.; Xie, Y.; Yi, N.; Huang, Y.; Chen, Y. Pyrolytic carbon-coated Si nanoparticles on elastic graphene framework as anode materials for high-performance lithium-ion batteries. *Carbon* **2015**, *82*, 161–167. [CrossRef]
31. Feng, K.; Ahn, W.; Lui, G.; Park, H.W.; Kashkooli, A.G.; Jiang, G.; Wang, X.; Xiao, X.; Chen, Z. Implementing an in-situ carbon network in Si/reduced graphene oxide for high performance lithium-ion battery anodes. *Nano Energy* **2016**, *19*, 187–197. [CrossRef]
32. Luo, Z.; Xiao, Q.; Lei, G.; Li, Z.; Tang, C. Si nanoparticles/graphene composite membrane for high performance silicon anode in lithium ion batteries. *Carbon* **2016**, *98*, 373–380. [CrossRef]
33. Wei, L.; Hou, Z.; Wei, H. Porous Sandwiched Graphene/Silicon Anodes for Lithium Storage. *Electrochim. Acta* **2017**, *229*, 445–451. [CrossRef]
34. Wu, L.; Yang, J.; Tang, J.; Ren, Y.; Nie, Y.; Zhou, X. Three-dimensional graphene nanosheets loaded with Si nanoparticles by in situ reduction of SiO_2 for lithium ion batteries. *Electrochim. Acta* **2016**, *190*, 628–635. [CrossRef]
35. Yao, W.; Chen, J.; Zhan, L.; Wang, Y.; Yang, S. Two-Dimensional Porous Sandwich-Like C/Si-Graphene-Si/C Nanosheets for Superior Lithium Storage. *ACS Appl. Mater. Interfaces* **2017**, *9*, 39371–39379. [CrossRef]
36. Younes, H.; Hong, H.; Peterson, G.P. A Novel Approach to Fabricate Carbon Nanomaterials–Nanoparticle Solids through Aqueous Solutions and Their Applications. *Nanomanuf. Metrol.* **2021**, *4*, 226–236. [CrossRef]
37. Younes, H.; Mao, M.; Sohel Murshed, S.M.; Lou, D.; Hong, H.; Peterson, G.P. Nanofluids: Key parameters to enhance thermal conductivity and its applications. *Appl. Therm. Eng.* **2022**, *207*, 118202. [CrossRef]
38. Hong, H.; Salem, D.; Christensen, G.; Yang, R. High Capacity Anodes. U.S. Patent 9,666,861B2, 30 May 2017.
39. Christensen, G.; Younes, H.; Hong, H.; Widener, C.; Hrabe, R.H.; Wu, J.J. Nanofluids as Media for High Capacity Anodes of Lithium-Ion Battery—A Review. *J. Nanofluids* **2019**, *8*, 657–670. [CrossRef]
40. Qu, E.; Chen, T.; Xiao, Q.; Lei, G.; Li, Z. Freestanding silicon/carbon nanofibers composite membrane as a flexible anode for Li-Ion battery. *J. Power Sources* **2018**, *403*, 103–108. [CrossRef]
41. Zhu, G.; Gu, Y.; Wang, Y.; Qu, Q.; Zheng, H. Neuron like Si-carbon nanotubes composite as a high-rate anode of lithium ion batteries. *J. Alloys Compd.* **2019**, *787*, 928–934. [CrossRef]
42. Li, J.-Y.; Xu, Q.; Li, G.; Yin, Y.-X.; Wan, L.-J.; Guo, Y.-G. Research progress regarding Si-based anode materials towards practical application in high energy density Li-ion batteries. *Mater. Chem. Front.* **2017**, *1*, 1691–1708. [CrossRef]